Biochar (2021) 3:175–188
https://doi.org/10.1007/s42773-020-00080-0

ORIGINAL RESEARCH

MgO-laden biochar enhances the immobilization of Cd/Pb in aqueous solution and contaminated soil

Yan Wang[1] · Lu Wang[1] · Zhangtao Li[1] · Dong Yang[1] · Jianming Xu[1] · Xingmei Liu[1]

Received: 10 September 2020 / Accepted: 24 November 2020 / Published online: 18 January 2021

Abstract

Great progress has been made in recent years to alleviate the heavy metal pollution, but the development of low-cost and eco-friendly adsorbents is still challenging. In this work, MgO-loaded biochar, as a potential adsorbent, was successfully synthesized via copyrolysis of corn straw and $MgCl_2$•$6H_2O$ at 600 ℃ and used for heavy metal immobilization in aqueous solution and contaminated soil. Nemerow pollution index and potential ecological risk index methods were also used to assess the potential ecological risk of the metals in soil after remediation. The results showed MgO-laden biochar exhibited a much higher Cd^{2+} adsorption capacity than the pristine biochar. Pseudo-second-order and Langmuir/Langmuir–Freundlich equations could describe the adsorption kinetics and isotherm of Cd^{2+} well. The maximum adsorption capacity of Cd^{2+} could reach to 1058.8 mg g^{-1} estimated by Langmuir–Freundlich equation. Cd^{2+} adsorption on MgO-laden biochar composite mainly involved the hydrolyzation of MgO, ionization of $Mg(OH)_2$ and precipitation of Cd^{2+} and OH^-. In addition, complexes with oxygen-containing groups and adsorption by $Mg(OH)_2$ also enhanced Cd immobilization. The result of soil-leaching test showed that the concentrations of TCLP-leaching (Toxicity Characteristic Leaching Procedure) Cd and Pb reduced by 22.4% and 29.0%, respectively, after 4% of MgO-laden biochar amendment, and the integrated pollution index and potential ecological risk decreased by 28.9% and 28.5%, respectively. These results suggest that MgO-laden corn straw biochar may be promising for application as a low-cost adsorbent for wastewater treatment and soil remediation.

Keywords MgO · Biochar · Cadmium · Lead · Pollution · Ecological risk

1 Introduction

Although the surface of the earth dominates with water, there is a shortage of potable water, and more than 1.2 billion people worldwide do not have access to clean drinking water (Bolisetty et al. 2019). Two and a half percent of fresh water was polluted by organic, inorganic, biological and macroscopic contaminants (Shaikh 2020). The industrial wastewater is one of the sources of the contaminants which often migrate into soil with irrigation. Soil and water pollution, that poses serious risks to human health is particularly true in developing countries such as India and China (Zhao et al. 2014). In 2014, the Chinese government published a national soil survey that showed that 16.1% of all soil sampling sites and 19.4% of arable soil sampling sites exceeded the soil standard (National Soil Survey 2014). It were reported that 2.786×10^9 m^2 of agricultural soils are polluted by Cd (Liu et al. 2015a). Unlike organic pollutants, heavy metals usually do not disappear over time in the natural environment, and can accumulate in the organism along with the food chain, causing human kidney damage and lower bone density, posing a threat to human and animal health (Jiang et al. 2012). Compared with other toxic metals such as Cu and Pb, Cd which is potentially toxic to biota at lower concentrations demonstrates greater mobility along the food chain and in the environment (He et al. 2015). Therefore, it is imperative to limit the transfer of Cd from wastewater to soils by reducing the Cd content in wastewater used for irrigation, and decrease the availability of Cd in soils by passivation.

Supplementary Information The online version contains supplementary material available at https://doi.org/10.1007/s42773-020-00080-0.

✉ Xingmei Liu
xmliu@zju.edu.cn

[1] Zhejiang Provincial Key Laboratory of Agricultural Resources and Environment, College of Environmental and Resource Sciences, Zhejiang University, Hangzhou 310058, China

To date, many methods have been used for the removal of heavy metals from aqueous systems including electrocoagulation, membrane filtration, ion-exchange, reverse osmosis, electrodialysis, solvent extraction and adsorption (Gunatilake 2015; Mahmood et al. 2011; Parmar and Thakur 2013). Among these methods, adsorption is considered to be the most efficient approach because of its simplicity and low cost of operation, highly efficient wastewater treatment and environmental friendliness (Mohan et al. 2014). However, most of commercially used adsorbents have high cost. The use of low-cost adsorbents such as biochar produced from the thermal degradation of the carbon-rich agricultural biomass is an alternative method for the removal of heavy metals. Recently, biochar has attracted increasing attention due to its important roles in carbon sequestration (Deng et al. 2017), pollutants removal (Nie et al. 2018; Tan et al. 2015) and soil fertility enhancement (Van Zwieten et al. 2010). Biochar derived from different feedstocks or produced under different conditions possesses various characteristics that directly affect its adsorption capacity for pollutants by controlling the surface functional groups, pore distribution, ash category (Ok et al. 2015; Rajapaksha et al. 2016) and redox capacity (Yuan et al. 2017). The heavy metal adsorption capacity of biochar is always lower than those of active carbon or other commercial adsorbents due to its limited amount of adsorption sites (Mohan et al. 2014). To date, an increasing number of studies have focused on the removal of toxic metals using biochar loaded with different minerals such as magnetite, hematite (γ-Fe_2O_3), zerovalent Fe (ZVI), hydrous Mn oxide and Fe–Mn oxides (Lu et al. 2016; Wang et al. 2016b, 2015). Magnesium oxide (MgO) is a nontoxic, low-cost and environment-friendly material produced from the naturally abundant and safe Mg element (Tian et al. 2017). It has been proved that MgO is a high-efficiency adsorbent for many types of pollutants such as phosphate, nitrate (Zhang et al. 2012), lead, cadmium (Cai et al. 2017; Chowdhury et al. 2016), nickel (Feng et al. 2015), fluoride (Jin et al. 2016b) and Congo red (Tian et al. 2013). Shen et al. (2019) reported that magnesium oxide (MgO)-coated corncob biochar reduced TCLP-leached lead from 10.63 to 5.24 mg L^{-1} (reduced by 50.71%). So here come the questions: could MgO-loaded biochar composite remove Cd efficiently in aqueous solutions? what's the mechanism? would co-existing Pb^{2+} affect the Cd removal? and what about the effect of MgO-loaded biochar composite on the availability of toxic metals in polluted soil? In this study, MgO-laden corn straw biochar composite was synthesized and used for the immobilization of Cd^{2+}/Pb^{2+} from aqueous solutions and co-contaminated soil. The objectives of this study are to (1) investigate the adsorption capability and mechanism of MgO-laden corn straw biochar for Cd^{2+}; (2) evaluate the ecological risks of heavy metals (Cd and Pb) in contaminated soils after remediation by MgO-laden biochar composite.

2 Materials and methods

2.1 Preparation of corn straw biochar and MgO-laden biochar

Corn straw biochar was produced by heating the sieved corn straw (particle size < 2 mm) in a tube furnace under nitrogen at a heating rate of 10 °C min^{-1} to reach 600 °C for 1 h. The MgO-laden biochar was prepared by mixing corn straw (particle size < 2 mm) with 2 mol L^{-1} of $MgCl_2{\cdot}6H_2O$ solution at a solid-to-liquid ratio of 1:7 g mL^{-1}. The suspension was placed in an ultrasonic vibration instrument for 30 min and then stirred intensely for 1.5 h at 25 °C. Then, the suspension was dried at 80 °C. The dry mixture of corn straw biomass and $MgCl_2{\cdot}6H_2O$ was heated to 600 °C for 1 h at 10 °C min^{-1} under N_2 flow. After cooling, the modified biochar was gently crushed and sieved through 40 mesh (< 0.425 mm) but not through 200 mesh and sealed in a container for further use (Shen et al. 2019; Zhang et al. 2012). In this study, the MgO was obtained at a high heating temperature. The MgO synthesis is based on the following reaction (Eq. 1).

$$MgCl_2 \cdot 6H_2O \rightarrow MgO + 2HCl \uparrow + 5H_2O \quad (1)$$

2.2 Evaluation of adsorption properties

MgO-laden biochar (1 mg or 10 mg) was weighed into a 50 mL plastic vessel, and then 20 mL of heavy metal solutions with different concentrations (10–1000 mg L^{-1}) were added into the vessels. After shaking for 24 h (25 °C) at 200 rpm, the liquid phase was filtered through nylon membrane filter with a pore size of 0.45 μm. After dilution with 1% HNO_3, the concentrations of the heavy metals and Mg^{2+} were determined by Inductively Coupled Plasma Mass Spectrometry (ICP-MS) (NexION 300X, PerkinElmer, USA) and Inductively Coupled Plasma Optical Emission Spectrometry (ICP-OES) (iCAP6300, Thermo, USA), respectively.

MgO-laden biochar (100 mg) was weighed into a 500 mL conical flask containing cadmium solutions (200 mL) with different concentrations. The adsorption kinetics test was carried out in a mechanical shaker at 25 °C with the rotation speed of 200 rpm. The liquid samples were collected at different intervals and filtered immediately. The concentration of the metal was determined by ICP-MS after dilution with 1% HNO_3.

The adsorption capacity (Q, mg g^{-1}) of the adsorbent was calculated using the following equation (Eq. 2):

$$Q = (C_0 - C_t) \times v/m \quad (2)$$

where v (L) is the volume of the Cd^{2+} solution, C_0 (mg L^{-1}) is the initial concentration of the Cd^{2+} solution, C_t (mg L^{-1}) is the concentration of the Cd^{2+} solution after adsorption at time t (min), and m (mg) is the mass of the adsorbent. All the experimental treatments were performed in duplicate and the average values were used as the results. Additional analyses were conducted whenever two measurements showed a difference larger than 5%.

2.3 Effect of initial pH and co-existing Pb^{2+} on the removal of Cd^{2+} by MgO-laden biochar

Solutions with several initial pH ranging from 2.0 to 8.0 were used in order to estimate the effect of pH on the removal of cadmium by the MgO-laden corn straw biochar in aqueous solutions. The pH values of the solutions (at different initial pH) with and without Cd^{2+} were determined using a pH meter after shaken for 24 h. To explore the tangible impact on the cadmium removal in wastewater, lead was selected as the co-existing metal. The adsorption isotherm and kinetics in the dual-metal system were studied. The initial concentrations of Cd^{2+} and Pb^{2+} ranged from 20 to 400 mg L^{-1}.

2.4 Biochar characterization before and after sorption of Cd^{2+}

To investigate the mechanism of Cd removal by MgO-laden corn straw biochar, the properties of MgO-laden biochar before and after cadmium adsorption were examined. The specific surface area of the biochar was measured by analyzing N_2 sorption at 77 K (Tristar 3020, Micromeritics Instrument Corp., USA). Prior to the adsorption of N_2, the biochar samples were vacuum degassed at 200 °C for 12 h. The specific surface area was calculated according to the Brunauer-Emmett Teller (BET) method. The micropore surface area and volume were calculated by the t-pot method. The surface morphology images of the biochar samples before and after Cd^{2+} adsorption were obtained using a scanning electron microscope combined with an energy dispersive X-ray detector (SEM–EDX, Quanta FEG650, FEI, USA). An X-ray diffractometer (XRD) (D8 Advance, Bruker, Germany) was employed to analyze the mineralogical characterization of the biochar samples at the 2θ angles in the 10°–80° range with Cu Kα radiation at a voltage of 40 kV and current of 40 mA, with a step size of 0.02° (Li et al. 2018). The functional groups present in the biochar were determined using a Fourier-Transform infrared (FTIR) spectrometer (Nicolet 6700, Thermo Fisher). FTIR spectra were obtained at a resolution of 4 cm^{-1} from 4000 to 500 cm^{-1} (Wang and Liu 2018). Biochar pH was determined after shaking a biochar sample (1 g) in deionized water (20 mL) for 1.5 h (Rajkovich et al. 2012). The C, H and N contents of the biochars were determined according to ASTM D 3176 using an elemental analyzer (Vario EL Cube, Elementar). And the oxygen values of biochars were calculated by difference. Ash contents of the biochars were determined according to ASTM D1782-84.

2.5 Soil sample collection and incubation experiments

The metals contaminated farmland soil with pH value of 5.12 was collected from Shangyu, Zhejiang province (N30.13°, E120.88°) around lead–zinc mining area. The soil was collected from 0 to 20 cm, mixed thoroughly, air-dried and ground to pass through 2 mm sieve. The Cd/Pb content was determined by ICP-MS (NexION300X, PerkinElmer, USA) after digested by HF-HNO_3 (3:1) using a microwave digestion system (MARS6, CEM, USA).The soil pH was measured using a pH meter (Seven Excellence TM, S470, Mettler Toledo, Switzerland) at a soil-to-water ratio of 1:2.5 (w/v) and the dissolved organic carbon (DOC) was extracted at a soil-to-water ratio of 1:5 (w/v) and measured by total organic carbon analysis (MULTI N/C 3100, Analytik Jena, GER).

Incubation experiments were carried out in plastic beakers to evaluate the effect of biochar and MgO-laden biochar on heavy metals availability. Different biochars were thoroughly mixed with 200 g soil at different ratios. Four treatments were as follows:

Control (CK, without remediation), 4% corn straw biochar amendment (w/w), 1% MgO-laden corn straw biochar amendment and 4% MgO-laden corn straw biochar amendment. Then, the soil samples were incubated at 25 °C and constant humidity (60% of water holding capacity) for 50 days.

2.6 Soil heavy metal availability and potential ecological risk assessment

Toxicity characteristic leaching procedure (TCLP) was often used to evaluate the activity of heavy metals in soils (Yu et al. 2014). In this study, TCLP method (EPA Method 1311) was used to extract the available toxic elements. Briefly, 1.5 g of soil was mixed with 30 mL of acetic acid solution (pH = 2.88). The supernatants were filtered and the concentrations of Pb and Cd were determined by ICP-MS after dilution. All tests were conducted in triplicate.

In this study, Nemerow pollution index (Nemerow 1971; Sun et al. 2006) and potential ecological risk index

(Hakanson 1980) were used to assess the ecological risk of toxic elements of soils treated with different amendments.

(1) Nemerow pollution index (NPI)

$$P_i = C_i/S_i \tag{3}$$

$$\mathrm{NPI} = \sqrt{\frac{P_{i\max}^2 + P_{i\mathrm{ave}}^2}{2}} \tag{4}$$

where P_i is single pollution index, C_i is toxic element concentration that TCLP extracted; S_i is the standard toxicity concentration (mg L^{-1}) of a contaminant (The contents of Pb and Cd are 5 and 0.5 mg kg^{-1}, respectively) (Gao et al. 2020; Sun et al. 2006); NPI is pollution index of multi-metals; $P_{i\max}$ is the maximum value of single pollution index, and $P_{i\mathrm{ave}}$ is the average value of single pollutant index.

(2) Potential ecological risk index (PI)

$$E_i = T_i \times P_i \tag{5}$$

$$\mathrm{PI} = \sum_{i=1}^{n} E_i \tag{6}$$

where E_i is monomial potential ecological risk index; T_i is the toxicity response coefficient of single heavy metal (Pb is 5 and Cd is 30) (Yu et al. 2014); P_i is single pollution index, PI is integrated potential ecological risk index of multi-metals.

3 Results and discussion

3.1 Adsorption properties

Figure S1 compares the equilibrium concentrations of Cd^{2+} after sorption by raw biochar and MgO-laden biochars (treated with different concentrations of $MgCl_2{\bullet}6H_2O$). The removal efficiency of Cd^{2+} by pristine biochar was far lower than those by the MgO-laden biochars. The equilibrium concentrations of Cd^{2+} in the solutions in which the MgO-laden biochars were added were below 0.03 mg L^{-1} when the initial Cd^{2+} level was 50 mg L^{-1}. Although the pH value of MgO-laden biochar (9.74) was not significantly changed compared to that of unmodified biochar (9.30), the buffering capacity was enhanced considerably (Wang et al. 2018). Therefore, greater amounts of Cd can be removed by precipitation after modification.

The adsorption isotherm was carried out in two different ranges of initial Cd^{2+} concentration including 10–80 mg L^{-1} and 50–800 mg L^{-1}. The biochar dose was 0.05 g L^{-1} and 0.5 g L^{-1}, respectively. Figure 1 shows the Langmuir, Freundlich and Langmuir–Freundlich adsorption isotherms

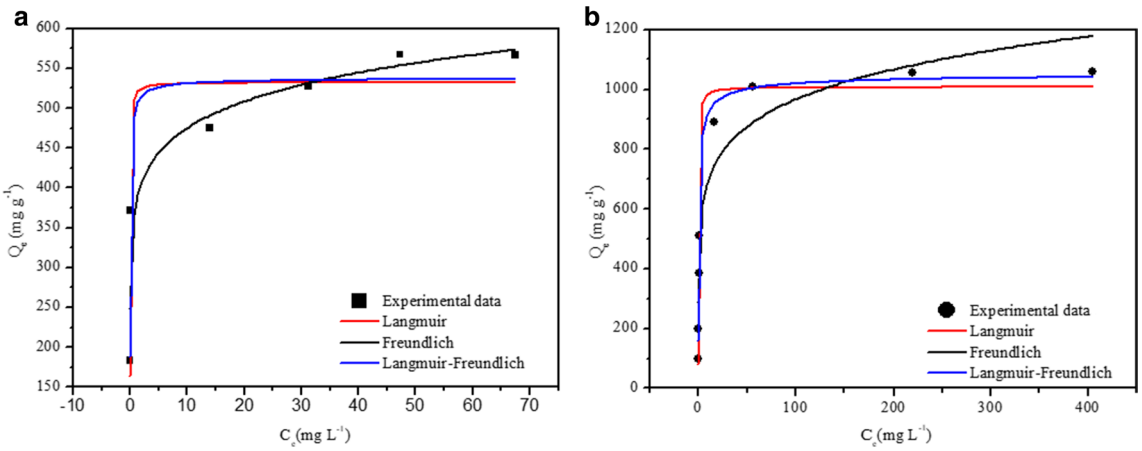

Fig. 1 Langmuir, Freundlich and Langmuir–Freundlich adsorption isotherms of Cd^{2+} on MgO-laden biochar (**a**, biochar dose 0.05 g L^{-1}; **b**, biochar dose 0.5 g L^{-1})

Table 1 The parameters from adsorption isotherm models

Biochar dose	Langmuir			Freundlich			Langmuir–Freundlich			
(g L^{-1})	Q_{max} (mg g^{-1})	k_l (L mg^{-1})	R^2	k_f (mg g^{-1})	n	R^2	Q_m (mg g^{-1})	k_a (L mg^{-1})	m	R^2
0.05	532.2	33.42	0.928	378.8	10.17	0.886	538.0	13.32	1.344	0.920
0.5	1007.7	4.464	0.973	503.4	7.056	0.887	1058.8	1.762	1.711	0.984

of Cd^{2+} on MgO-laden biochar and the fitting parameters are listed in Table 1. The adsorption data fitted Langmuir model ($R^2 = 0.928/0.973$) better than Freundlich model ($R^2 = 0.886/0.887$) for both systems, and $k_1 = 33.419 >> 1$, which suggested that surface coverage plays the dominant role in the adsorption of Cd^{2+}. When the biochar dose increased from 0.05 to 0.5 g L^{-1}, the maximum adsorption capacity values increased from 532.17 to 1007.7 mg g^{-1} estimated by Langmuir equation. It is summarized that the adsorption capacity for Cd^{2+} by modified biochar ranged in 22.22–322.6 mg g^{-1} (Wang et al. 2019), which is far lower than the data in this study. The adsorption fitted Langmuir–Freundlich model best and $m = 1.711 > 1$ when the biochar dose was 0.5 g L^{-1}, suggesting that the adsorbent was heterogeneous and Cd^{2+} adsorption by MgO-laden biochar was diffusion-controlled at low metal concentration, while monomolecular adsorption occurred with a saturation value at high metal concentration (Mohan et al. 2011).

Increasing the adsorbent dose improved the maximum adsorption capacity. To explain these observations, the pH was determined after the adsorption of different concentrations of Cd^{2+} (Fig. 2). In the system with higher Cd^{2+} concentration, the pH value of the solution decreased with increasing initial Cd^{2+} concentration after adsorption because that an increasing amount of hydroxyl ions were combined with Cd^{2+}. In the system with lower concentration of Cd^{2+}, the solution pH first decreased sharply, and then decreased slightly and remained at approximately 8.1 at last. Compared to the pH value of the solution with a lower biochar dose (0.05 g L^{-1}) and lower concentration of Cd^{2+}, the pH value of the solution with a dose of 0.5 g L^{-1} and larger Cd^{2+} concentration was higher. A higher pH will lead to increased binding of Cd^{2+} due to the increase of OH^- concentration. Therefore, a higher adsorption capacity was observed in the system with a higher dose of MgO-laden biochar. The OH^- originated in the ionization of the $Mg(OH)_2$ which generated when the MgO-laden biochar came in contact with water. The reaction in this process is described by the following equations:

$$MgO + H_2O \rightarrow Mg(OH)_2 \downarrow \quad (7)$$

$$Mg(OH)_2 \rightarrow Mg^{2+} + 2OH^- \quad (8)$$

Figure 3 demonstrates that the increase in the Mg^{2+} concentration was consistent with the decrease in the Cd^{2+} concentration in the solution, and the Mg^{2+} concentration increased with the increase with the increases in the initial

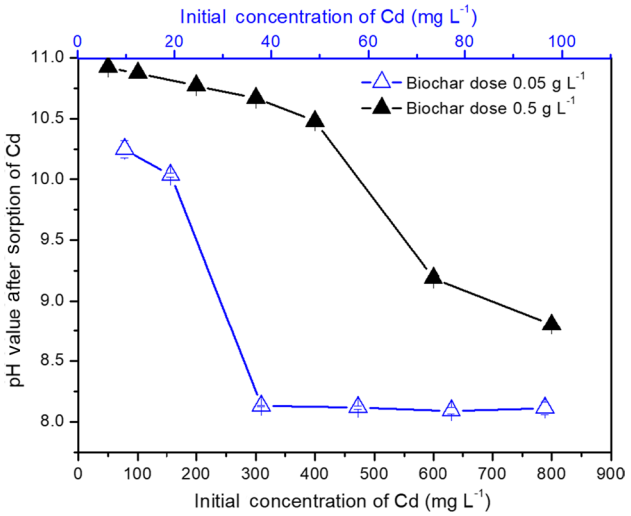

Fig. 2 pH values of the solutions after adsorption of different concentrations of Cd^{2+} within different ranges of concentration at two adsorbent dose levels

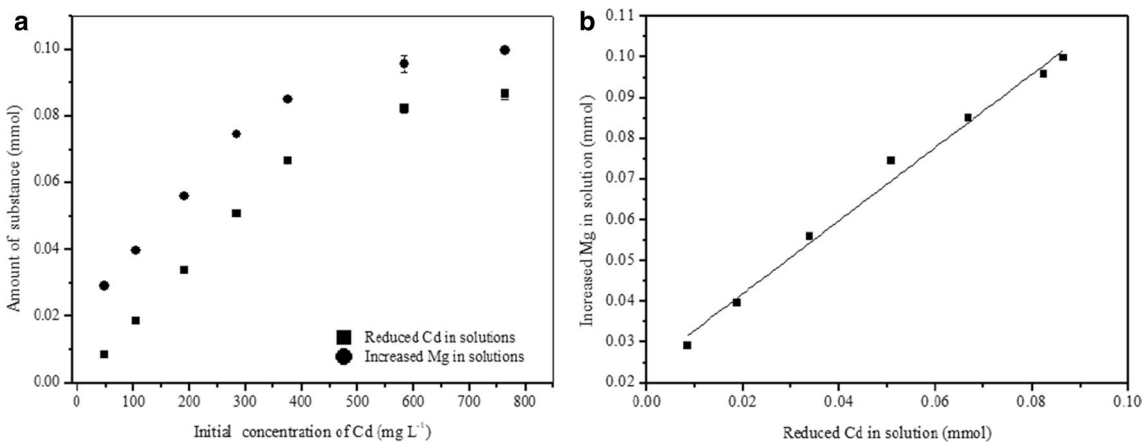

Fig. 3 Molar concentration changes (**a**) and correlation (**b**) of the reduction in the Cd^{2+} concentration and the increase in the Mg^{2+} concentration in the solution after adsorbing different concentrations of Cd^{2+}

concentration of Cd^{2+}, which suggested that more Mg^{2+} were exchanged with the Cd^{2+} as the concentration of Cd^{2+} increased, promoting greater transfer of Cd^{2+} from the solution to the adsorbent. Recent historical studies have shown that Mg contents in cereal seeds have markedly declined over time, and two thirds of people surveyed in developed countries received less than their minimum daily requirement of Mg (Guo et al. 2016). Thus, the release of magnesium into the environment accompanying the capture of a toxic element will be a win–win situation. The pH decreased with increasing Cd^{2+} concentration (Fig. 2), suggesting an increasing consumption of OH^-. Therefore, Cd^{2+} might be bound with OH^- to generate $Cd(OH)_2$ or $Cd(OH)^+$. The correlation coefficient between the reduction in Cd^{2+} concentration and the increase in Mg^{2+} concentration was 0.988, indicating that the presence of Cd^{2+} in the solution promoted the release of Mg^{2+}. This chemical reaction is described by Eq. 9. It means that the amount of Cd^{2+} that exchanged with Mg^{2+} should be the same in theory. The content of MgO in composite is 0.5642 mg g^{-1}. If all the Mg exchanged with Cd^{2+}, the amount of Cd that grabbed by the composite should be 1006 mg g^{-1}, which was a bit lower than the experiment data, because that biochar matrix also could adsorb small amounts of Cd^{2+}, and the other reason was that MgO and its hydration products $Mg(OH)_2$ can also aid the removal of heavy metals through physical sorption, cation exchange, and complexation (Jin et al. 2016a). Therefore, MgO-corn straw biochar composite is rather promising used for Cd^{2+} removal.

$$MgO + H_2O + Cd^{2+} \rightarrow Mg^{2+} + Cd(OH)_2 \downarrow \quad (9)$$

Adsorption kinetic models are often used to explain the adsorption process and investigate the rate control mechanism of the removal of toxic metal ions from the aqueous phase by various absorbents. First, the effect of the contact time on the removal of Cd^{2+} by MgO-laden corn straw biochar in solutions with the initial concentrations of Cd^{2+} ranging from 19 to 168 mg L^{-1} was studied. Figure S2 demonstrates that the sorption rate of Cd^{2+} increased initially, and then achieved adsorption equilibrium. More than 98% of Cd^{2+} in the solutions with various initial concentrations in the 19–168 mg L^{-1} range were removed by MgO-laden biochar. The adsorption equilibrium was reached more rapidly for lower Cd^{2+} level in solution. The adsorption equilibrium time increased with increasing initial Cd^{2+} level. For example, only 40 min were required to remove 98% of Cd^{2+} for the initial Cd^{2+} level of 19 mg L^{-1}, while approximately 120 min were necessary for the removal of 98% of Cd^{2+} when the initial Cd^{2+} level was changed to 48 mg L^{-1}.

The results of the fits to the pseudo-first order, pseudo-second order and intraparticle diffusion kinetic models of Cd^{2+} adsorption on MgO-laden biochar are presented in Fig. 4 and the corresponding parameters are listed in Table 2. At a low initial Cd^{2+} level (19 mg L^{-1}), pseudo-first-order and pseudo-second-order equations could describe the adsorption well ($R^2 = 0.999/0.979$), while the intra-particle diffusion equation failed to describe the adsorption. As the initial Cd^{2+} concentration increased from 48 to 168 mg g^{-1}, the correlation coefficient of the intraparticle diffusion equation increased from 0.966 to 0.993, and the sorption rate constant changed also in a narrow range from 9.791 to 13.70 mg g^{-1} min^{-1} and the line did not pass through the origin, suggesting tha adsorption or sort of boundary layer was controlled by intraparticle diffusion at an initial concentration in a range of 48–168 mg g^{-1}, but the adsorption was not the only rate-limiting step, and the sorption rate was limited or combined with other steps (Kumar et al. 2018). The sorption rate constant showed no dependence

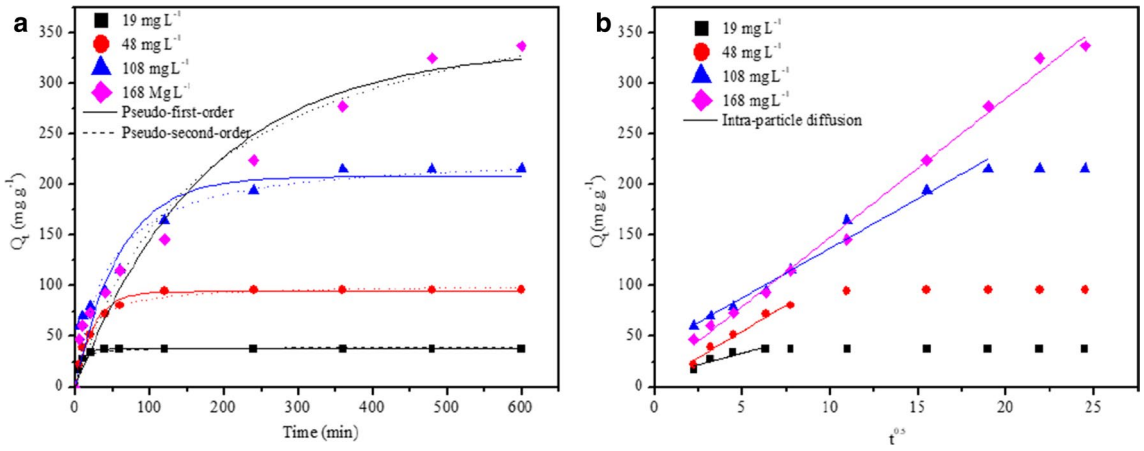

Fig. 4 **a** Sorption kinetics of Cd^{2+} at different concentrations on MgO-laden biochar. **b** Cd^{2+} sorption data fitted by the intraparticle diffusion model (biochar dose was 0.5 g L^{-1})

Table 2 The parameters from adsorption kinetics models

	Pseudo-first-order			Pseudo-second-order			Intra-particle diffusion		
C_0 (mg L^{-1})	Q_e (mg g^{-1})	k_1 (min^{-1})	R^2	Q_e (mg g^{-1})	k_2 (g mg^{-1} min^{-1})	R^2	k_3 (mg g^{-1} $min^{0.5}$)	b (mg g^{-1})	R^2
19	37.83	0.127	0.999	39.37	5.520×10^{-3}	0.979	4.671	10.38	0.768
48	94.47	0.0410	0.987	101.2	5.974×10^{-4}	0.994	10.44	3.200	0.966
108	208.2	0.0169	0.911	230.1	1.029×10^{-4}	0.946	9.791	39.54	0.976
168	334.8	0.0057	0.943	420.7	1.386×10^{-5}	0.957	13.70	11.24	0.993

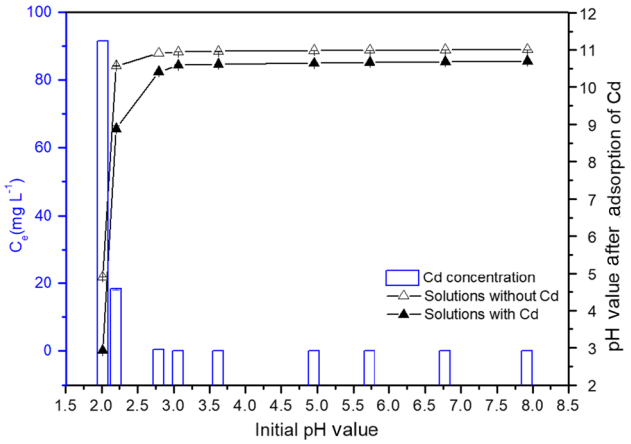

Fig. 5 The effect of initial pH on the Cd^{2+} removal by MgO-laden biochar from aqueous solutions (initial concentration of Cd^{2+} was 92 mg L^{-1}; biochar dose was 0.5 g L^{-1})

on the initial Cd^{2+} concentration. When the initial Cd^{2+} concentration ranged from 48 to 168 mg L^{-1}, the pseudo-second-order model could also describe the adsorption process well ($R^2 = 0.957–0.994$) and the sorption rate constant (k_2) decreased with the increasing initial Cd^{2+} concentration. The metal adsorption kinetic evaluation of biomass-based sorbent mostly conformed to the pseudo-second-order model (Akpomie and Conradie 2020; Tao et al. 2019). The pseudo-second-order equation is based on the assumption that the rate-limiting process is chemisorption or physicochemical adsorption including electron transfer and exchange or bond formation (Li 2019). Therefore, the adsorption of Cd^{2+} onto the MgO-laden biochar is due to either chemisorption or physicochemical adsorption.

3.2 Effect of initial pH and coexisting Pb^{2+} on Cd^{2+} removal from aqueous solutions by MgO-laden biochar

The effect of pH on the Cd^{2+} adsorption onto MgO-laden biochar was observed in the pH range of 2.0–8.0 (Fig. 5). Various initial pH values of solutions with and without Cd^{2+} were adjusted by HCl (0.1 M) and NaOH (0.1 M) solutions at the beginning of the adsorption. After shaking for 24 h, the pH of the solution with and without Cd^{2+} (only with adsorbent) showed a pronounced increase. However, compared to the solutions without Cd^{2+}, the pH values of the solution with Cd^{2+} were lower, suggesting that the pH decreased after Cd^{2+} adsorption. When the initial pH was 2.0, the pH of the solution without Cd^{2+} changed to 4.90 after shaking for 24 h and changed to 2.92 after the adsorption of Cd^{2+}, and the removal rate of Cd^{2+} was rather low. However, the removal rate reached 81.5% when the initial pH was 2.2. After adsorption, the concentration of Cd^{2+} in solutions ranged from 0.03 to 0.06 mg L^{-1} when the initial pH was in the 3.0–7.0 range. To summarize, the Cd^{2+} removal by MgO-laden biochar was pH dependent, and the adsorbent changed the solutions pH by the hydrolyzation reaction of MgO and kept the solution alkaline, improving the precipitation of Cd^{2+}.

In wastewater, Cd^{2+} always co-exists with other metal ions. Compared to other metal ions, Pb^{2+} is more likely to affect the removal of Cd^{2+} due to its smaller hydrated radius (4.01 Å) and solubility product constant (K_{sp}) that will give rise to a greater affinity for most functional groups and OH^- (Park et al. 2016). Here, we assumed that the concentrations of Pb^{2+} and Cd^{2+} in the solution system were the same. In fact, the situation is more complicated in industrial wastewater. Figure 6 shows the adsorption kinetics (a) and isotherms (b) of mixed ions. The adsorption equilibrium time of Cd^{2+} was delayed from 360 to 480 min, and the maximum adsorption capacity was decreased. The Cd^{2+} adsorption isotherm was best fitted by the Langmuir model ($R^2 = 0.947$), and the maximum Cd^{2+} adsorption capacity of 401.85 mg g^{-1} was estimated by the Langmuir model. Therefore, it is concluded that more adsorbent is required in the presence of Pb^{2+} coexisting in the system.

3.3 Changes of MgO-laden biochar characteristics before and after Cd^{2+} adsorption

To investigate the mechanism of Cd^{2+} removal by MgO-laden biochar, SEM–EDS, XRD and FTIR were used to detect the characteristics of pristine biochar, modified biochar and modified biochar after Cd^{2+} sorption.

Table S1 lists the pH, ultimate composition and pore characteristics of corn straw biochar and modified biochar.

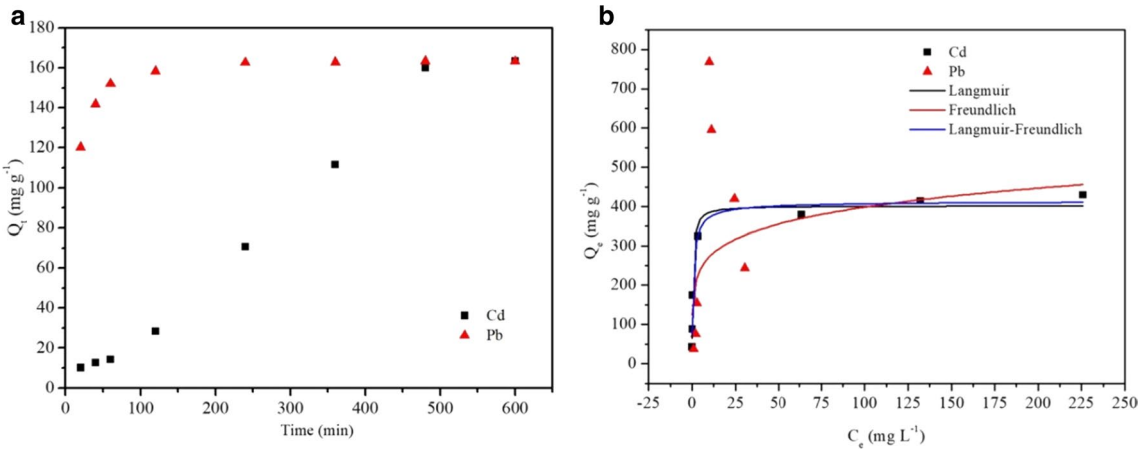

Fig. 6 Kinetics (**a**) and isotherms (**b**) of mixed ions adsorption on MgO-laden biochar (biochar dose, 0.5 g L^{-1}; concentrations of Cd^{2+} and Pb^{2+} were 80 mg L^{-1})

After modification, the biochar pH, ash and oxygen contents increased but the special surface area (SSA) calculated by the BET method decreased from 135.91 to 38.32 m^2 g^{-1} and the pore width changed strongly. Previous study also found that surface areas of MgO-coated magnetic sugarcane harvest residue biochars decreased from 118 to 27.2 m^2 g^{-1} with Mg content increased from 2.12% to 20.47% (Shen et al. 2019). The average pore width increased from 1.9 to 5.6 nm. Cai et al. (2017) reported that highly active and commercial MgO particles have the BET surface areas of 47.85 and 5.26 m^2 g^{-1}, and average pore diameters of 12.15 and 30.36 nm, respectively. SEM images showed that different size of particles distributed on the biochar surface and the pores of the biochar were filled by the particles (Fig. 7), which was relative to the ultrasonic treatment. It was reported that the $MgCl_2$ with the ultrasonic impregnation method may produce large aggregates during pyrolysis, which may result in the heterogeneity of Mg-containing minerals on biochar and the blockage of biochar pores after synthesis (Zhang et al. 2020). That is why the specific surface area decreased after Mg impregnation.

Figure 7 shows that the surface of the raw biochar was smooth with many pores and few particles that were identified as KCl crystals by XRD (Fig. 9). After modification using $MgCl_2{\cdot}6H_2O$, the surface of the biochar became rough and heterogeneous, and the nanoscale and microsized particles were filled in the pores and on the surface of the biochar, so that the specific surface area decreased from 135.91 to 38.32 m^2 g^{-1}; however, the adsorption capacity was enhanced. Therefore, the physical adsorption by pores does not dominate the sorption process. After adsorption, the concentration of Cd^{2+} in the solution decreased drastically, and many spindly particles were generated, suggesting that new Cd-containing particles were generated, achieving the transfer of Cd from solution to the adsorbent.

The elementary composition (Fig. 8 and Table S2) of the particles on the surface of the modified biochar and postsorption biochar was analyzed use a SEM–EDX. After Cd^{2+} adsorption, the atom fraction of magnesium decreased from 31.09% to 3.46% and the atom fraction of oxygen only decreased slightly, but the atom fraction of cadmium increased from 0 to 35.03%, verifying the transfer of Mg from the adsorbent to the solution and the transfer of Cd from the solution to the adsorbent. In addition, there were almost no changes in the atom fractions of carbon and chlorine. Therefore, the most likely reactions were the hydrolyzation of MgO particles on the surface of biochar and then Mg^{2+} and OH^- were released to the solution due to the ionization of $Mg(OH)_2$. The released OH^- and Cd^{2+} in the solution finally combined to generate $Cd(OH)_2$, because that the K_{sp} of $Cd(OH)_2$ is smaller than that of $Mg(OH)_2$; this is consistent with the results of the adsorption tests. On the other hand, the generation of $Cd(OH)_2$ promoted the ionization of $Mg(OH)_2$.

The result of XRD patterns of biochars (Fig. 9) suggested that only KCl crystal was detected in the corn straw biochar. After the modification, the MgO crystal generated, which was consistent with the SEM–EDX result. Therefore, the solid particles on the surface of the biochar (SEM) were MgO. After sorption of Cd^{2+}, the intensity of MgO decreased from approximately 1700 to 350 and Mg $(OH)_2$ crystals were generated, suggesting the hydrolyzation of MgO. Although Cd was detected in the biochar surface by SEM–EDX, no clear peaks involving Cd-related crystal was observed. It is possible that the structures of the Cd $(OH)_2$ particles adhering to the biochar surface or in the pores were amorphous. The lack of Cd-related crystal may be due to the destruction of the $Cd(OH)_2$ crystals by the biochar matrix, because for the pure MgO nanoparticles, $Cd(OH)_2$ and CdO

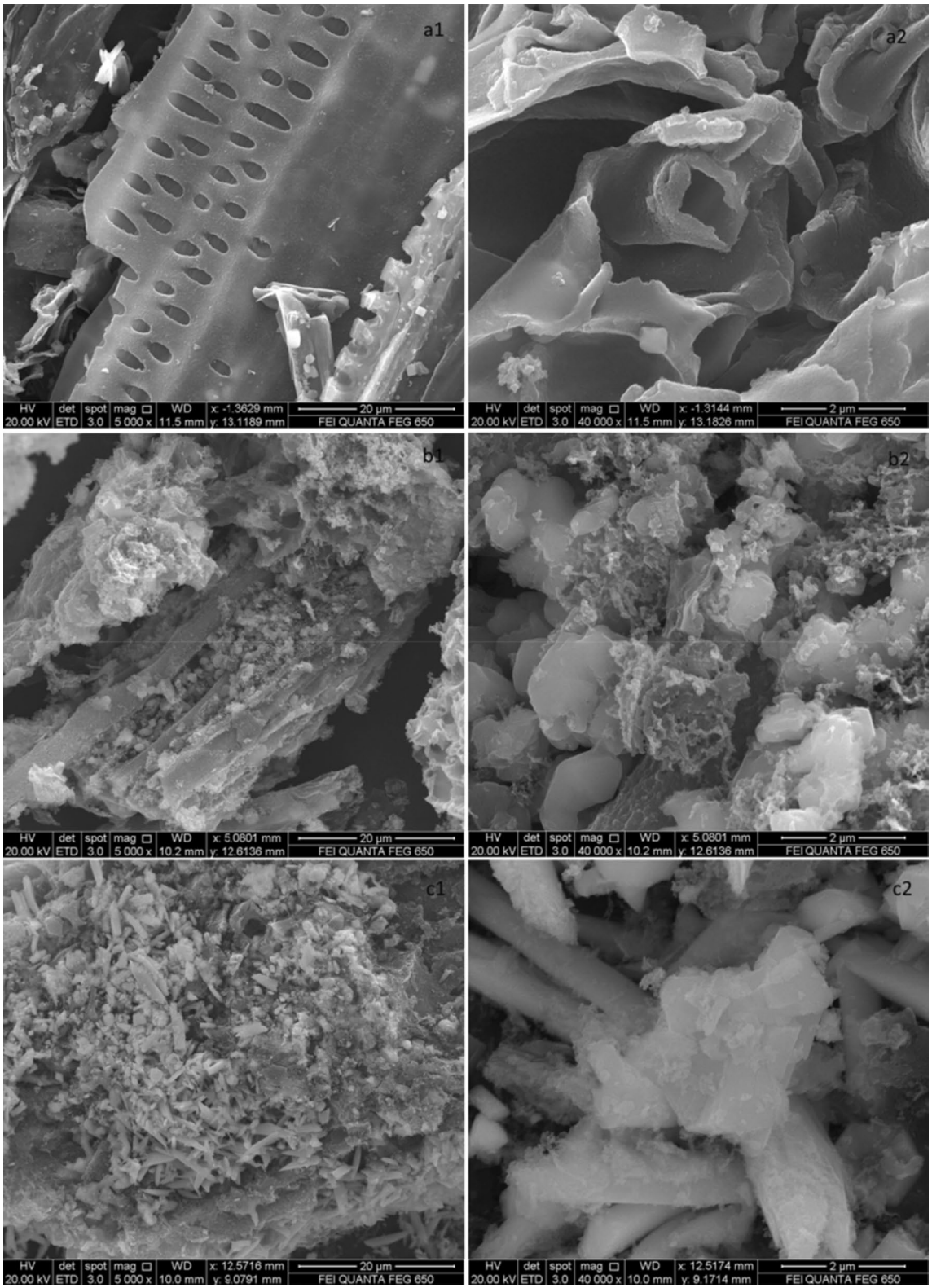

Fig. 7 SEM micrographs of **a** corn straw biochar, **b** MgO-laden corn straw biochar and **c** MgO-laden corn straw biochar after sorption of Cd^{2+} at different magnifications

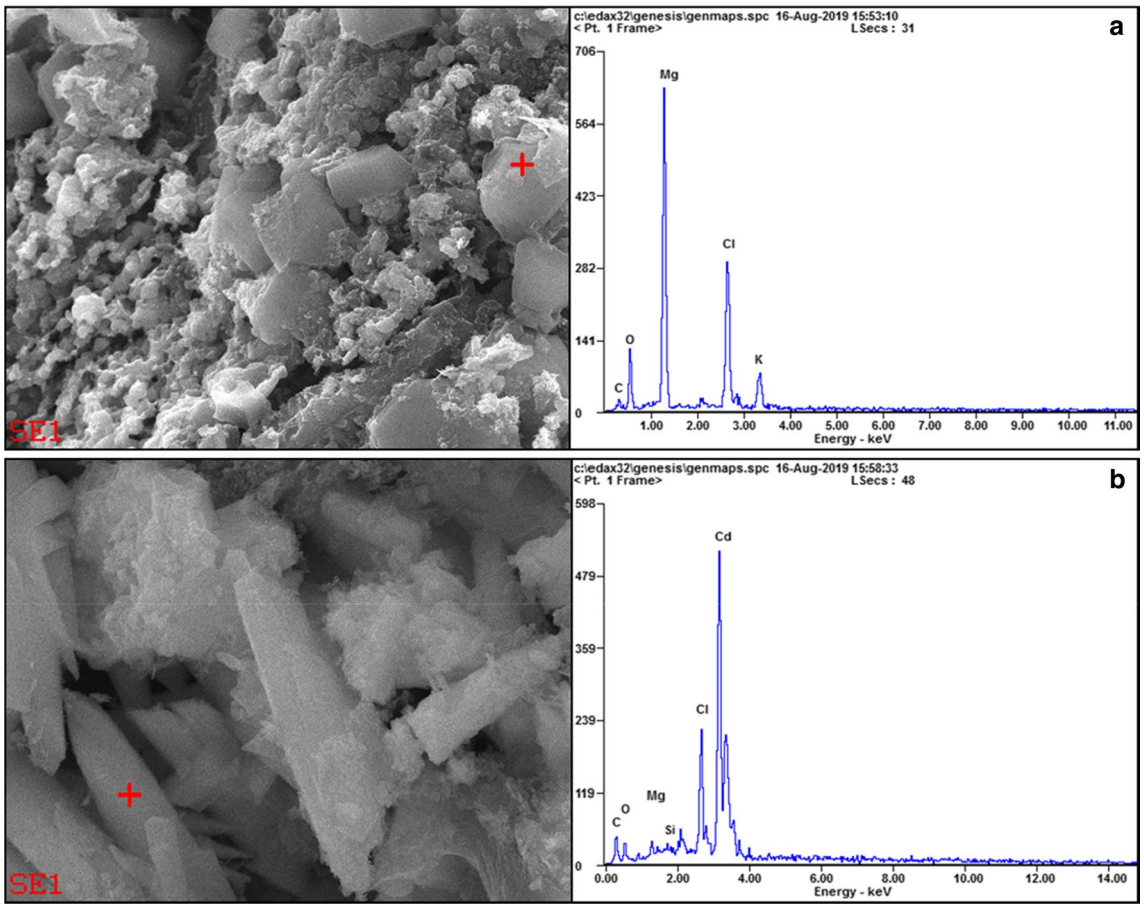

Fig. 8 SEM–EDX of **a** MgO-laden biochar, **b** postadsorbed biochar

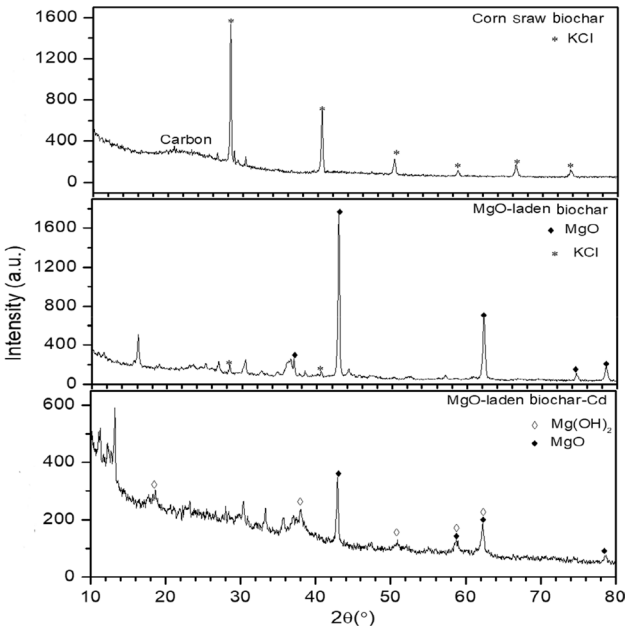

Fig. 9 XRD patterns of biochars

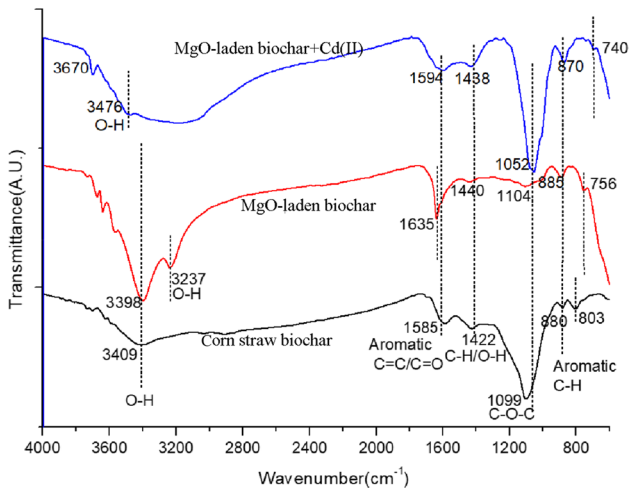

Fig. 10 FTIR spectra of biochars

crystals can be identified by XRD after Cd^{2+} sorption (Cai et al. 2017).

The FTIR spectra of corn straw biochar, and MgO-laden biochar before and after Cd^{2+} adsorption are shown in Fig. 10. For corn straw biochar, the peaks at 3398–3476 cm^{-1} (H-bonded O–H stretching vibrations of hydroxyl groups of phenols, alcohols, and organic acids) (Keiluweit et al. 2010) were observed. The peaks at 1585 cm^{-1} and 1099 cm^{-1} were assigned as C=C/C=O stretching vibrations and C–O–C vibrations (Chi et al. 2017; Wang et al. 2016a). The peaks at 740–885 cm^{-1} were frequently observed from corn straw biochar and other biochars and are due to the out-of-plane deformation of aromatic C–H (Wang and Liu 2017).

After modification, the peaks at 3409 cm^{-1} changed to 3398 cm^{-1} and the peak intensity increased; however, the peak intensity decreased after adsorption of Cd^{2+}, suggesting that O–H functional groups were bound with Cd^{2+}. Moreover, a new peak at 3237 cm^{-1} corresponding to free OH^- that may be generated by the hydrolyzation of MgO appeared after the modification, and it disappeared after the sorption of Cd^{2+}. In addition, the modified biochar showed a pronounced band at 1635 cm^{-1} due to the protein carboxyl C=O groups (Liu et al. 2015b), and the position of the peak shifted to 1594 cm^{-1} after sorption, indicating that the carboxyl on the surface of the biochar was complexed with Cd^{2+}. The coverage of micron- and nano-sized MgO particles gave rise to the disappearance of the peak at 1099 cm^{-1} after the modification and the peak appeared after Cd^{2+} sorption; however, the peak position changed from 1099 cm^{-1} to 1052 cm^{-1}, because the hydrolyzation reaction of MgO, the ionization reaction of $Mg(OH)_2$ and the precipitation reaction between Cd^{2+} and hydroxyl led to the exposure of the C–O–C functional groups, which then complexed with the remaining Cd^{2+}.

3.4 Effect of different biochars' addition on toxic element activity in soil and potential ecological risk assessment based on TCLP leaching

The paddy soil properties which are listed in Table S3 have been described in previous research (Li et al. 2020). The total contents of Cd and Pb in the paddy soil severely exceeded the class II standard for agriculture land of China (NEPA 2018). The effect of corn straw biochar and MgO-laden biochar on TCLP-leaching (a) lead and (b) cadmium is shown in Fig. 11. The results showed that adding corn straw biochar and MgO-laden biochar decreased the concentrations of TCLP-leaching Cd and Pb. TCLP-leaching Cd in soils only reduced by 0.6%, and TCLP-leaching Pb reduced 19.3% after treated with 4% corn straw biochar, because that the active site on the biochar surface was occupied by Pb^{2+} which had a smaller hydrated ionic radius (Park et al. 2016) and a higher concentration in this soil. MgO-laden biochar presented more effective in Cd and Pb immobilization than pristine biochar, which might be because that MgO-laden biochar increased soil pH more obviously. The soil pH was 6.2 and 7.7 after treated with 4% of biochar and 1% MgO-laden biochar, respectively. And Cd and Pb are easily sequestrated at a higher pH value. Therefore, MgO-laden biochar was more effective to sequestrate Cd^{2+} and Pb^{2+}. The concentrations of TCLP-leaching Cd and Pb decreased with the addition rate of MgO-laden biochar increasing. Similarly, the Pb^{2+} was easier to be sequestrated by MgO-laden biochar than Cd^{2+} due to the smaller solubility product constant of $Pb(OH)_2$, which was consistent with the result of the adsorption test in aqueous solution. Adding 1% of MgO-laden biochar only reduced 7.0% of TCLP-leaching Cd, but TCLP-leaching Pb reduced 21.8%. Adding 4% of MgO-laden biochar decreased the concentrations of TCLP-leaching Cd and Pb by 22.4% and 29.0%, respectively. Previous study also

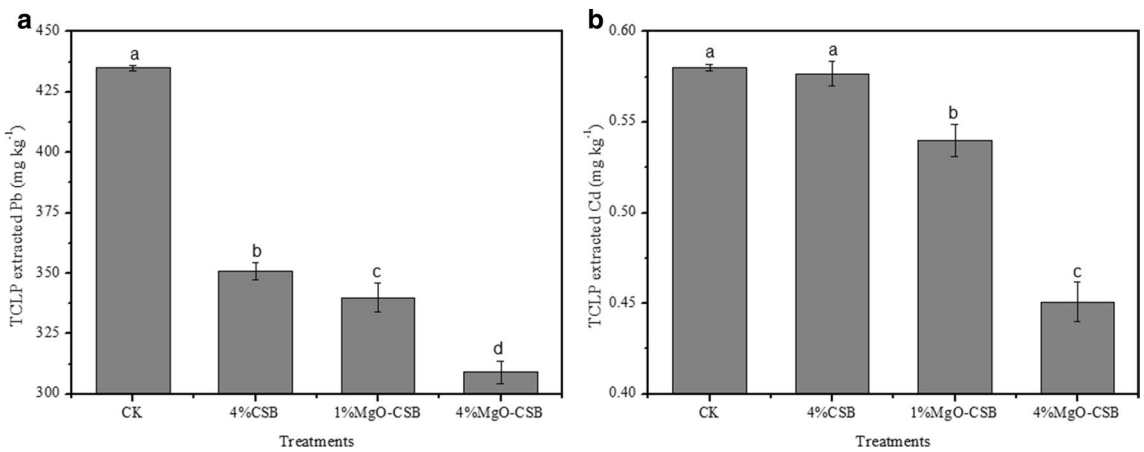

Fig. 11 Effect of corn straw biochar and MgO-laden biochar on TCLP-leaching **a** lead and **b** cadmium

Table 3 Nemerrow pollution index and Potential ecological risk index of heavy metals in soil (CSB means 'corn straw biochar', MgO-CSB means 'MgO-laden corn straw biochar')

Treatments	Toxic elements	Nemerrow pollution index		Potential ecological risk index	
		P_i	NPI	E_i	PI
CK	Cd	1.16	68.96	34.82	469.77
	Pb	86.99		434.94	
4% CSB	Cd	1.15	55.65	34.61	385.40
	Pb	70.16		350.79	
1% MgO-CSB	Cd	1.08	53.93	32.39	372.37
	Pb	67.99		339.97	
4% MgO-CSB	Cd	0.90	49.00	27.05	336.07
	Pb	61.80		309.01	

reported that MgO-coated biochar could reduce TCLP-leached Pb (Shen et al. 2019).

Potential ecological risk was assessed by Nemerow pollution index (NPI) and Potential ecological risk index (RI). Table 3 lists the calculation results of Nemerrow pollution index and Potential ecological risk index. Table S4 lists the classification of index. The results showed that biochar or MgO-laden biochar addition decreased the P_i (Cd) and P_i (Pb), and single pollution index of Cd decreased from 1.16 to 0.9 after 4% MgO-laden biochar amendment, which suggested that the Cd pollution rank decreased from low polluted to warning limit level. The values of NPI reflected the integrated pollution status of the total heavy metals. The NPI decreased by 28.9% after 4% of MgO-laden biochar application.

The potential ecological risk index was often used to assess the potential ecological risk of single and multi-pollutants in the environment. The results showed the order of E_i value was Pb > Cd, and the ecological risk of Cd was low (E_i (Cd) < 40). The value of E_i (Pb) was between 300 and 600, suggested that the ecological risk of Pb was high at this soil sample collection site. Both corn straw biochar and MgO-laden biochar addition decreased the E_i (Cd), E_i (Pb) and the comprehensive pollution status (PI) of the two toxic metals. However, MgO-laden biochar presented more efficient in Cd and Pb immobilization than unmodified biochar. Adding 4% of MgO-laden biochar, the value of E_i (Pb) decreased from 434.94 to 309.01, which means that the risk of Pb lowered by one rank, and the PI also decreased from 469.77 to 336.07.

4 Conclusions

In summary, MgO loading enhanced Cd removal in aqueous solution by precipitation with OH^- that was released via the ionization of Mg $(OH)_2$ derived from the MgO hydrolysis on the surface of biochar. In addition to precipitation, the adsorption also involved other mechanisms such as complexation with oxygen-containing functional groups and electrostatic adsorption. The maximum adsorption capacity of Cd^{2+} was 1058.8 mg g^{-1}, but a larger dose is required when there are other coexisting toxic metals like Pb^{2+} in the system. Adding MgO-laden corn straw biochar into contaminated soil could enhance the immobilization and decrease the potential ecological risks of Cd and Pb assessed by NPI. Considering its advantages of low cost, high adsorption capacity and environmental friendliness, MgO-laden biochar is promising for $Cd^{2+}$and Pb^{2+} immobilization in wastewater and contaminated soil.

Acknowledgements This work was funded by the National Natural Science Foundation of China (no. 41907102) and the Postdoctoral Science Foundation of China (no. 2019M662068).

References

Akpomie KG, Conradie J (2020) Advances in application of cotton-based adsorbents for heavy metals trapping, surface modifications and future perspectives. Ecotoxicol Environ Saf. https://doi.org/10.1016/j.ecoenv.2020.110825

Bolisetty S, Peydayesh M, Mezzenga R (2019) Sustainable technologies for water purification from heavy metals: review and analysis. Chem Soc Rev 48:463–487. https://doi.org/10.1039/c8cs00493e

Cai Y, Li C, Wu D, Wang W, Tan F, Wang X, Wong PK, Qiao X (2017) Highly active MgO nanoparticles for simultaneous bacterial inactivation and heavy metal removal from aqueous solution. Chem Eng J 312:158–166. https://doi.org/10.1016/j.cej.2016.11.134

Chi T, Zuo J, Liu F (2017) Performance and mechanism for cadmium and lead adsorption from water and soil by corn straw biochar. Front Environ Sci Eng 11:15. https://doi.org/10.1007/s11783-017-0921-y

Chowdhury IH, Chowdhury AH, Bose P, Mandal S, Naskar MK (2016) Effect of anion type on the synthesis of mesoporous nanostructured MgO, and its excellent adsorption capacity for the removal of toxic heavy metal ions from water. RSC Adv 6:6038–6047. https://doi.org/10.1039/c5ra16837f

Deng W, Van Zwieten L, Lin Z, Liu X, Sarmah AK, Wang H (2017) Sugarcane bagasse biochars impact respiration and greenhouse gas emissions from a latosol. J Soil Sediment 17:632–640. https://doi.org/10.1007/s11368-015-1347-4

Feng J, Zou L, Wang Y, Li B, He X, Fan Z, Ren Y, Lv Y, Zhang M, Chen D (2015) Synthesis of high surface area, mesoporous MgO nanosheets with excellent adsorption capability for Ni (II) via a distillation treating. J Colloid Interface Sci 438:259–267. https://doi.org/10.1016/j.jcis.2014.10.004

Gao R et al (2020) Remediation of Pb, Cd, and Cu contaminated soil by co-pyrolysis biochar derived from rape straw and orthophosphate: speciation transformation, risk evaluation and mechanism inquiry. Sci Total Environ 730:139119. https://doi.org/10.1016/j.scitotenv.2020.139119

Gunatilake S (2015) Methods of removing heavy metals from industrial wastewater. Methods 1:14. http://jmess.org/wp-content/uploads/2015/11/JMESSP13420004.pdf

Guo W, Nazim H, Liang Z, Yang D (2016) Magnesium deficiency in plants: an urgent problem. Crop J 4:83–91. https://doi.org/10.1016/j.cj.2015.11.003

Hakanson L (1980) An ecological risk index for aquatic pollution control. A sedimentological approach. Water Res 14:975–1001. https://doi.org/10.1016/0043-1354(80)90143-8

He S, He Z, Yang X, Stoffella PJ, Baligar VC (2015) Soil biogeochemistry, plant physiology, and phytoremediation of cadmium-contaminated soils. Advances in Agronomy, vol 134. Elsevier, Berlin, pp 135–225

Jiang J, Xu R, Jiang T, Li Z (2012) Immobilization of Cu (II), Pb (II) and Cd (II) by the addition of rice straw derived biochar to a simulated polluted Ultisol. J Hazard Mater 229:145–150. https://doi.org/10.1016/j.jhazmat.2012.05.086

Jin F, Wang F, Al-Tabbaa A (2016a) Three-year performance of in-situ solidified/stabilised soil using novel MgO-bearing binders. Chemosphere 144:681–688. https://doi.org/10.1016/j.chemosphere.2015.09.046

Jin Z, Jia Y, Zhang K, Kong L, Sun B, Shen W, Meng F, Liu J (2016b) Effective removal of fluoride by porous MgO nanoplates and its adsorption mechanism. J Alloys Compd 675:292–300. https://doi.org/10.1016/j.jallcom.2016.03.118

Keiluweit M, Nico PS, Johnson MG, Kleber M (2010) Dynamic molecular structure of plant biomass-derived black carbon (biochar). Environ Sci Technol 44:1247–1253. https://doi.org/10.1021/es9031419

Kumar PS, Varjani SJ, Suganya S (2018) Treatment of dye wastewater using an ultrasonic aided nanoparticle stacked activated carbon: kinetic and isotherm modelling. Bioresour Technol 250:716–722. https://doi.org/10.1016/j.biortech.2017.11.097

Li X (2019) Preparation and adsorption properties of biochar/g-C3N4 composites for methylene blue in aqueous solution. J Nanomater. https://doi.org/10.1155/2019/2394184

Li Z, Wang L, Meng J, Liu X, Xu J, Wang F, Brookes P (2018) Zeolite-supported nanoscale zero-valent iron: new findings on simultaneous adsorption of Cd (II), Pb (II), and As (III) in aqueous solution and soil. J Hazard Mater 344:1–11. https://doi.org/10.1016/j.jhazmat.2017.09.036

Li Z, Wang L, Wu J, Xu Y, Wang F, Tang X, Ok YS, Xu J, Liu X et al (2020) Zeolite-supported nanoscale zero-valent iron for immobilization of cadmium, lead, and arsenic in farmland soils: Encapsulation mechanisms and indigenous microbial responses. Environ Pollut. https://doi.org/10.1016/j.envpol.2020.114098

Liu F, Liu X, Ding C, Wu L (2015a) The dynamic simulation of rice growth parameters under cadmium stress with the assimilation of multi-period spectral indices and crop model. Field Crop Res 183:225–234. https://doi.org/10.1016/j.fcr.2015.08.004

Liu Y, He Z, Uchimiya M (2015b) Comparison of biochar formation from various agricultural by-products using FTIR spectroscopy. Modern Appl Sci 9:246

Lu H, Wang J, Ferguson S, Wang T, Bao Y, Hao H (2016) Mechanism, synthesis and modification of nano zerovalent iron in water treatment. Nanoscale 8:9962–9975. https://doi.org/10.1039/c6nr00740f

Mahmood T, Saddique M, Naeem A, Mustafa S, Dilara B, Raza Z (2011) Cation exchange removal of Cd from aqueous solution by NiO. J Hazard Mater 185:824–828. https://doi.org/10.1016/j.jhazmat.2010.09.094

Mohan D, Rajput S, Singh VK, Steele PH, Pittman CU Jr (2011) Modeling and evaluation of chromium remediation from water using low cost bio-char, a green adsorbent. J Hazard Mater 188:319–333. https://doi.org/10.1016/j.jhazmat.2011.01.127

Mohan D, Sarswat A, Ok YS, Pittman CU Jr (2014) Organic and inorganic contaminants removal from water with biochar, a renewable, low cost and sustainable adsorbent–a critical review. Bioresour Technol 160:191–202. https://doi.org/10.1016/j.biortech.2014.01.120

National Soil Survey, (2014) Ministry of environmental protection of the People's Republic of China. http://www.mee.gov.cn/gkml/sthjbgw/qt/201404/t20140417_270670.htm

Nemerow NL (1971) Benefits of water quality enhancement. Syracuse University, Syracuse, NY, Report No. 16110 DAJ, prepared for the US EPA

NEPA (2018) Environmental quality standard for soil contamination of agricultural land (GB15618-2018). In: National Environmental Protection Agency of China

Nie C, Yang X, Niazi NK, Xu X, Wen Y, Rinklebe J, Ok YS, Xu S, Wang H (2018) Impact of sugarcane bagasse-derived biochar on heavy metal availability and microbial activity: a field study. Chemosphere 200:274–282. https://doi.org/10.1016/j.chemosphere.2018.02.134

Ok YS, Uchimiya SM, Chang SX, Bolan N (2015) Biochar: Production, characterization, and applications. CRC Press, Boca Raton

Park JH, Ok YS, Kim SH, Cho JS, Heo JS, Delaune RD, Seo DC (2016) Competitive adsorption of heavy metals onto sesame straw biochar in aqueous solutions. Chemosphere 142:77–83. https://doi.org/10.1016/j.chemosphere.2015.05.093

Parmar M, Thakur LS (2013) Heavy metal Cu, Ni and Zn: toxicity, health hazards and their removal techniques by low cost adsorbents: a short overview. Int J Plant Sci 3:143–157

Rajapaksha AU, Chen SS, Tsang DCW, Zhang M, Vithanage M, Mandal S, Gao B, Bolan NS (2016) Engineered/designer biochar for contaminant removal/immobilization from soil and water: potential and implication of biochar modification. Chemosphere 148:276–291. https://doi.org/10.1016/j.chemosphere.2016.01.043

Rajkovich S, Enders A, Hanley K, Hyland C, Zimmerman AR, Lehmann J (2012) Corn growth and nitrogen nutrition after additions of biochars with varying properties to a temperate soil. Biol Fertil Soils 48:271–284. https://doi.org/10.1007/s00374-011-0624-7

Shaikh TMA (2020) Adsorption of Pb(II) from wastewater by natural and synthetic adsorbents. Biointerface Res Appl Chem 10:6522–6539. https://doi.org/10.33263/briac105.65226539

Shen Z, Zhang J, Hou D, Tsang DC, Ok YS, Alessi DS (2019) Synthesis of MgO-coated corncob biochar and its application in lead stabilization in a soil washing residue. Environ Int 122:357–362

Sun Y, Xie Z, Li J, Xu J, Chen Z, Naidu R (2006) Assessment of toxicity of heavy metal contaminated soils by the toxicity characteristic leaching procedure. Environ Geochem Hlth 28:73–78

Tan X, Liu Y, Zeng G, Wang X, Hu X, Gu Y, Yang Z (2015) Application of biochar for the removal of pollutants from aqueous solutions. Chemosphere 125:70–85. https://doi.org/10.1016/j.chemosphere.2014.12.058

Tao Q, Chen Y, Zhao J, Li B, Li Y, Tao S, Li M, Li Q, Xu Q, Li Y, Li H, Li B, Chen Y, Wang C (2019) Enhanced Cd removal from aqueous solution by biologically modified biochar derived from digestion residue of corn straw silage. Sci Total Environ 674:213–222. https://doi.org/10.1016/j.scitotenv.2019.03.438

Tian P, Han X, Ning G, Fang H, Ye J, Gong W, Lin Y (2013) Synthesis of porous hierarchical MgO and its superb adsorption properties. ACS Appl Mater Inter 5:12411–12418. https://doi.org/10.1021/am403352y

Tian G, Wang W, Zong L, Wang A (2017) MgO/palygorskite adsorbent derived from natural Mg-rich brine and palygorskite for high-efficient removal of Cd (II) and Zn (II) ions. J Environ Chem Eng 5:1027–1036. https://doi.org/10.1016/j.jece.2017.01.028

Van Zwieten L, Kimber S, Morris S, Chan KY, Downie A, Rust J, Joseph S, Cowie A (2010) Effects of biochar from slow

pyrolysis of papermill waste on agronomic performance and soil fertility. Plant Soil 327:235–246. https://doi.org/10.1007/s11104-009-0050-x

Wang Y, Liu R (2017) Comparison of characteristics of twenty-one types of biochar and their ability to remove multi-heavy metals and methylene blue in solution. Fuel Process Technol 160:55–63

Wang Y, Liu R (2018) H_2O_2 treatment enhanced the heavy metals removal by manure biochar in aqueous solutions. Sci Total Environ 628:1139–1148. https://doi.org/10.1016/j.scitotenv.2018.02.137

Wang S, Gao B, Zimmerman AR, Li Y, Ma L, Harris WG, Migliaccio KW (2015) Removal of arsenic by magnetic biochar prepared from pinewood and natural hematite. Bioresour Technol 175:391–395. https://doi.org/10.1016/j.biortech.2014.10.104

Wang C, Gu L, Liu X, Zhang X, Cao L, Hu X (2016a) Sorption behavior of Cr (VI) on pineapple-peel-derived biochar and the influence of coexisting pyrene. Int Biodeterior Biodegrad 111:78–84. https://doi.org/10.1016/j.ibiod.2016.04.029

Wang S, Gao B, Li Y (2016b) Enhanced arsenic removal by biochar modified with nickel (Ni) and manganese (Mn) oxyhydroxides. J Ind Eng Chem 37:361–365. https://doi.org/10.1016/j.jiec.2016.03.048

Wang L, Yu K, Jiang S et al (2018) Low-carbon and low-alkalinity stabilization/solidification of high-Pb contaminated soil. Chem Eng J 351:418–427. https://doi.org/10.1016/j.cej.2018.06.118

Wang L, Wang YJ, Ma F, Tankpa V, Bai SS, Guo XM, Wang X (2019) Mechanisms and reutilization of modified biochar used for removal of heavy metals from wastewater: a review. Sci Total Environ 668:1298–1309. https://doi.org/10.1016/j.scitotenv.2019.03.011

Yu B, Wang Y, Zhou Q (2014) Human health risk assessment based on toxicity characteristic leaching procedure and simple bioaccessibility extraction test of toxic metals in urban street dust of Tianjin. China PLoS ONE. https://doi.org/10.1371/journal.pone.0092459

Yuan Y, Bolan N, Prévoteau A, Vithanage M, Biswas JK, Ok YS, Wang H (2017) Applications of biochar in redox-mediated reactions. Bioresour Technol 246:271–281. https://doi.org/10.1016/j.biortech.2017.06.154

Zhang M, Gao B, Yao Y, Xue Y, Inyang M (2012) Synthesis of porous MgO-biochar nanocomposites for removal of phosphate and nitrate from aqueous solutions. Chem Eng J 210:26–32. https://doi.org/10.1016/j.cej.2012.08.052

Zhang J, Hou D, Shen Z, Jin F, O'Connor D, Pan S, Ok YS, Tsang DCW, Bolan NS, Alessi DS (2020) Effects of excessive impregnation, magnesium content, and pyrolysis temperature on MgO-coated watermelon rind biochar and its lead removal capacity. Environ Res. https://doi.org/10.1016/j.envres.2020.109152

Zhao F, Ma Y, Zhu Y, Tang Z, McGrath SP (2014) Soil contamination in China: current status and mitigation strategies. Environ Sci Technol 49:750–759. https://doi.org/10.1021/es5047099